Accepted Manuscript

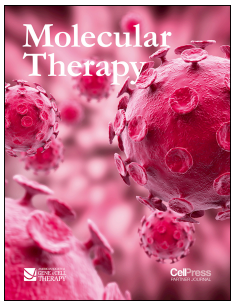

Development of targeted siRNA nanocomplexes to prevent fibrosis in experimental glaucoma filtration surgery

Owen Fernando, Aristides D. Tagalakis, Sahar Awwad, Steve Brocchini, Peng T. Khaw, Stephen L. Hart, Cynthia Yu-Wai-Man

PII: S1525-0016(18)30445-3

DOI: 10.1016/j.ymthe.2018.09.004

Reference: YMTHE 4743

To appear in: *Molecular Therapy*

Received Date: 16 May 2018

Accepted Date: 5 September 2018

Please cite this article as: Fernando O, Tagalakis AD, Awwad S, Brocchini S, Khaw PT, Hart SL, Yu-Wai-Man C, Development of targeted siRNA nanocomplexes to prevent fibrosis in experimental glaucoma filtration surgery, *Molecular Therapy* (2018), doi: 10.1016/j.ymthe.2018.09.004.

Development of targeted siRNA nanocomplexes to prevent fibrosis in experimental glaucoma filtration surgery

Owen Fernando[3†], Aristides D. Tagalakis[3,5†], Sahar Awwad[1,2,4], Steve Brocchini[1,2,4], Peng T. Khaw[1,2], Stephen L. Hart[3], Cynthia Yu-Wai-Man[1,2*]

1. National Institute for Health Research (NIHR) Biomedical Research Centre at Moorfields Eye Hospital NHS Foundation Trust and UCL Institute of Ophthalmology, London, EC1V 2PD, United Kingdom.
2. UCL Institute of Ophthalmology, London, EC1V 9EL, United Kingdom.
3. Experimental and Personalised Medicine Section, Genetics and Genomic Medicine Programme, UCL Great Ormond Street Institute of Child Health, London, WC1N 1EH, United Kingdom.
4. UCL School of Pharmacy, London, WC1N 1AX, United Kingdom.
5. Department of Biology, Edge Hill University, Ormskirk, L39 4QP, United Kingdom.

Keywords: Nanoparticle, siRNA, targeting peptide, glaucoma, fibrosis

Short title: siRNA nanocomplexes prevent fibrosis in glaucoma

† Authors have contributed equally

Corresponding Author:

Dr Cynthia Yu-Wai-Man

UCL Institute of Ophthalmology, 11-43 Bath Street, London EC1V 9EL, UK.

Tel: +44 20 7608 6887; Fax: +44 20 7608 6887

E-mail: c.yu-wai-man@ucl.ac.uk

Abstract

RNA interference induced by double-stranded, small interfering RNA (siRNA) molecules has attracted great attention as a naturally-occurring approach to silence gene expression with high specificity. The Myocardin-Related Transcription Factor/Serum Response Factor (MRTF/SRF) pathway is a master regulator of cytoskeletal gene expression and thus represents a promising target to prevent fibrosis. A major hurdle to implementing siRNA therapies is the method of delivery and we have thus optimised lipid-peptide-siRNA (LPR) nanoparticles containing MRTF-B siRNAs as a targeted approach to prevent conjunctival fibrosis. We tested fifteen LPR nanoparticle formulations with different lipid compositions, surface charges and targeting or non-targeting peptides in human conjunctival fibroblasts. *In vitro*, the LPR formulation of DOTMA/DOPE lipid with the targeting peptide Y (LYR) was the most efficient in *MRTF-B* gene silencing and non-cytotoxic compared to the non-targeting formulation. *In vivo*, subconjunctival administration of LYR nanoparticles containing MRTF-B siRNAs doubled bleb survival in a pre-clinical rabbit model of glaucoma filtration surgery. Furthermore, MRTF-B LYR nanoparticles reduced the *MRTF-B* mRNA by 29.6% in rabbit conjunctival tissues, which led to significantly decreased conjunctival scarring with no adverse side effects. LYR-mediated delivery of siRNA shows promising results to increase bleb survival and to prevent conjunctival fibrosis after glaucoma filtration surgery.

1. Introduction

Glaucoma is the leading cause of irreversible blindness in the world, currently affecting over 60 million people worldwide, and estimated to rise to 76 million by 2020 and nearly 112 million by 2040.[1] Postoperative subconjunctival and episcleral fibrosis represent the critical determinant of the long-term surgical outcome and intraocular pressure after glaucoma filtration surgery (GFS).[2] Mitomycin-C (MMC) is an antimetabolite drug that is used to modulate wound healing in glaucoma surgery, and acts by inhibiting DNA synthesis and causing widespread apoptosis.[3] Serious vision-threatening side effects have been associated with the use of MMC, namely a 5% risk of hypotonous maculopathy,[4] severe infection,[5] corneal melting and perforation,[6] and scleral calcification.[7] In addition, some patients still scar and fail surgery despite antimetabolite therapy. There is thus a large unmet need for alternative agents with more targeted physiological effects and less cytotoxicity.

Serum response factor (SRF) is a ubiquitous transcription factor and a master regulator of cytoskeletal gene expression,[8,9] including many genes involved in fibrosis.[10-12] The Myocardin-Related Transcription Factor (MRTF) family is one of the principal families of signal-regulated SRF co-activators.[9,13] The two MRTF family members, MRTF-A and MRTF-B, are regulated by cytoskeletal dynamics and respond to variations in the cellular concentration of G-actin, to which they bind through N-terminal RPEL motifs.[14,15] The MRTF/SRF pathway plays a key role in myofibroblast activation and has been linked to ocular,[16-19] vascular,[10] skin[11] and lung fibrosis.[12]

Small interfering RNAs (siRNAs) are double-stranded RNA molecules 20-25 nucleotides long that regulate gene expression by degrading messenger RNA targets specifically, thereby leading to gene silencing.[20] We have previously shown that cationic lipid (L)- peptide (P)- siRNA (R) nanocomplexes (LPR) represent an efficient delivery system for *MRTF-B* gene silencing in human conjunctival fibroblasts.[18] The LPR formulation used *in vitro* may not be suitable for *in vivo* application as cationic nanocomplexes can display poor tissue penetration, cause non-specific

binding to cells, interact with serum proteins and lead to inflammation. Unlike cationic nanocomplexes, anionic nanocomplexes are resistant to aggregation in the presence of serum[21] and can achieve significant gene silencing in delivering siRNA.[22] Cholesterol is a non-charged helper lipid that plays a role in many cellular membrane-related events, such as membrane fusion and endocytosis, and introducing cholesterol as a component of certain DNA/RNA carriers can increase their hydrophobic stability and improve transfection *in vivo* compared to carriers not containing cholesterol.[23,24] PEGylation can also reduce aggregation due to binding of serum proteins and can increase the receptor-targeted specificity. In the case of anionic nanocomplexes, PEGylation can further enhance the transfection efficiency in cells.[21] We thus optimised LPR formulations by varying the lipid composition to confer different surface properties, including surface charge and PEGylation to enhance their *in vivo* biocompatibility. We also evaluated the peptide targeting specificity in LPR nanocomplexes in transfections of human conjunctival fibroblasts. Finally, we investigated the safety and efficacy of MRTF-B siRNA delivered by targeted LPR nanoparticles on bleb survival and conjunctival scarring in a pre-clinical rabbit model of GFS.

2. Results

2.1. Development and biophysical characterisation of cationic and anionic nanoparticles

We developed and characterised fifteen LPR formulations using three types of liposomes [DD (DOTMA/DOPE), DC (DOTMA/DOPE + cholesterol), DA (anionic DOPG/DOPE + PEG)], five types of peptides [targeting (Y, ME27, KG31, KG32), non-targeting (ME72)], and siRNA [R]. LPRs containing DD had a mean size of 119.5 ± 7.3 (SEM) nm (Figure 1A). Targeting DD/Y/R (108.3 ± 6.4 nm) and DD/ME27/R (89.9 ± 2.7 nm) nanoparticles were similar in size to the non-targeting DD/ME72/R (99.7 ± 3.4 nm). Targeting DD/KG31/R (163.1 ± 2.5 nm) and DD/KG32/R (136.6 ± 1.7 nm) nanoparticles were slightly larger in size. LPRs containing anionic DOPG/DOPE + PEG lipid (DA) had a mean size of 102.1 ± 2.4 nm and were similar in size to DD-containing LPRs. However, LPRs containing DOTMA/DOPE + cholesterol lipid (DC) were significantly larger in size (234.7 ± 11.0 nm) than LPRs containing DD or DA.

LPRs containing DD and DC were strongly cationic and had a mean charge of +51.5 ± 1.7 (SEM) mV and + 63.7 ± 1.8 mV, respectively, whereas LPRs containing DA were anionic (-44.4 ± 3.6 mV) (Figure 1B). LPRs containing DD and DA nanoparticles also had relatively low polydispersity indices (PDI) of 0.37 ± 0.01 and 0.25 ± 0.02, respectively (Figure 1C). However, DC-containing LPRs had a high PDI of 0.84 ± 0.05. PDIs greater than 0.3 are indicative of multiple populations rather than the ideal monodisperse population. All LPR nanoparticle formulations were spherical in morphology using negative-staining TEM (Figure 1D). The bigger size of DC-containing LPRs compared to those containing DD or DA was also verified by TEM.

2.2. Enhanced silencing effect in human conjunctival fibroblasts transfected with receptor-targeted nanoparticles

For LPRs containing DD, the silencing efficiency on the *MRTF-B* gene in human conjunctival fibroblasts was significantly increased with the use of targeting peptides (Y: 52.7%, *p*

= 0.002; ME27: 49.1%, p = 0.0006; KG31: 55.4%, p = 0.0002; KG32: 53.5%, p = 0.004) compared to the non-targeting peptide (ME72: 38.1%, p = 0.014) (Figure 2A). Similarly, for LPRs containing DC, the silencing efficiency of the *MRTF-B* gene was also significantly higher with the use of targeting peptides (Y: 41.8%, p = 0.011; ME27: 52.1%, p = 0.022; KG31: 54.1%, p = 0.002; KG32: 45.1%, p = 0.0006) compared to the non-targeting peptide (ME72: 23.7%, p = 0.002) (Figure 2B). There were statistically significant differences in the *MRTF-B* gene expression between the ME27 and ME72 peptide containing LPR formulations with DD (p = 0.020) (Figure 2A) and with DC (p = 0.002) (Figure 2B). ME72 contains a scrambled sequence of the ME27 targeting ligand and this result thus supports the targeting effect of the ME27 peptide. However, targeting and non-targeting DA-containing LPRs did not have any statistically significant effect on *MRTF-B* gene silencing in human conjunctival fibroblasts (Figure 2C).

2.3. Receptor-targeted LYR nanoparticles display low cytotoxicity in human conjunctival fibroblasts

For LPRs containing DD, none of the MRTF-B siRNA loaded nanoparticles were cytotoxic in human conjunctival fibroblasts compared to control nanoparticles or untreated cells (Figure 3A). There was a statistically significant decrease in cell viability for LPRs containing DC-peptide ME27-control siRNA (p = 0.007), DC-peptide ME72-control siRNA (p = 0.041), DC-peptide KG31-control siRNA (p = 0.001), and DC-peptide KG31-MRTF-B siRNA (p = 0.008) (Figure 3B).

For LPRs containing DA, there was also no statistically significant decrease in cell viability in human conjunctival fibroblasts compared to untreated cells, except for DA-peptide ME27-MRTFB siRNA (p = 0.004) (Figure 3C). Our results show that the cationic LPR formulation of DOTMA/DOPE with the targeting peptide Y (LYR) was the most efficient in *MRTF-B* gene silencing (52.7 ± 2.7 %) and the least cytotoxic in human conjunctival fibroblasts, therefore, this formulation was used in all subsequent experiments.

2.4. Biophysical characterisation and silencing effect of LYR nanoparticles in rabbit conjunctival fibroblasts

The LYR nanoparticles containing control and rabbit MRTF-B siRNAs had a mean size of 128.8 ± 1.7 (SEM) nm and 134.9 ± 4.3 nm, respectively (Figure 4A). The LYR nanoparticles containing control siRNA (35.0 ± 3.1 mV) and rabbit MRTF-B siRNA (48.7 ± 1.9 mV) were both strongly cationic (Figure 4B). The PDIs were 0.36 ± 0.01 and 0.41 ± 0.01 for control LYR and rabbit MRTF-B LYR nanoparticles, respectively, indicating that the populations were not monodisperse. MRTF-B LYR nanoparticles decreased *MRTF-B* gene expression in rabbit conjunctival fibroblasts by 41.5% ($p = 0.018$) compared to control LYR nanoparticles (Figure 4C). MRTF-B LYR nanoparticles also did not have any significant effect on cell viability in rabbit conjunctival fibroblasts compared to control LYR nanoparticles ($p = 0.168$) (Figure 4D).

2.5. *In vivo* administration of LYR nanoparticles increases the long-term success of surgery in a rabbit model of glaucoma filtration surgery

We used an established and clinically validated rabbit model of experimental GFS to investigate the effects of LYR nanoparticles containing MRTF-B siRNA on wound healing in the conjunctiva.[25,26] Subconjunctival scarring after GFS is one of the most aggressive models of scar tissue formation, and failure of surgery is due to excessive scarring. A bleb arises when a filtration cannula is inserted during the surgery and drains aqueous fluid from the anterior chamber of the eye to under the conjunctiva (Figure 5A). The primary efficacy end-point was bleb survival as this is indicative of the long-term opening of the filtration pathway created during surgery. Bleb failure was defined as the appearance of a flat, scarred and vascularised bleb associated with a deep anterior chamber. We tested the LYR formulation *in vivo* as it was non-cytotoxic and the most efficient in terms of *MRTF-B* gene silencing in human conjunctival fibroblasts. Bleb survival was doubled from 11.0 ± 0.6 (SEM) days for control LYR nanoparticles to 22.0 ± 2.1 days for MRTF-B

LYR nanoparticles (p = 0.005), and to 22.5 ± 1.3 days for mitomycin-C (p = 0.001) (Figures 5B and 5C).

2.6. LYR nanoparticles decrease conjunctival scarring and do not cause any local or systemic side effects

The MRTF-B LYR nanoparticles significantly decreased the scar tissue formation in the rabbit conjunctiva compared to control nanoparticles (Figure 6A). Total cellularity also remained significantly increased in the control LYR nanoparticles group compared to the MRTF-B LYR nanoparticles (Figure 6B). In addition, MRTF-B LYR nanoparticles decreased the expression of αSMA by cells, suggesting the presence of fewer myofibroblasts (Figure 6C). Newly-laid extracellular matrix and collagen were present to a greater degree in the control LYR nanoparticles group compared to the MRTF-B LYR nanoparticles (Figure 6D).

We further tested the silencing effect of MRTF-B LYR nanoparticles on *MRTF-B* gene expression *in vivo* in rabbit conjunctival tissues. MRTF-B LYR nanoparticles decreased the *MRTF-B* gene expression by 29.6% in rabbit conjunctival tissues compared to control LYR nanoparticles (p = 0.046) (Figure 7A). MRTF-B LYR nanoparticles also decreased the *ACTA2* gene expression in rabbit conjunctival tissues compared to control LYR nanoparticles, however this was not statistically significant (p = 0.535) (Figure 7B). In addition, none of the rabbits showed any signs of ocular or systemic toxicity during the study.

3. Discussion

This study demonstrates proof-of-concept that *MRTF-B* targeting by small interfering RNA is an effective application of genetic inhibition to prolong bleb survival and to prevent conjunctival fibrosis after experimental GFS. Moreover, we have shown that the MRTF-B siRNA-loaded nanoparticles are safe to use *in vivo* in the conjunctiva and do not lead to any local or systemic adverse side effects. Our previous studies have also shown that direct injection is an efficient route of administration of nanoparticles, for example direct injection into subcutaneous tumours[27,28] and convection enhanced delivery through a cannula directly into the brain.[21,29]

Potential advantages of nanoparticle-mediated siRNA therapy over drugs, such as MMC, include its cell specificity, potency and duration.[30] There has been increasing interest in developing siRNA-based therapeutics in herpetic stromal keratitis,[31] retinoblastoma,[32] ocular inflammation,[33] non-arteritic anterior ischemic optic neuropathy,[34] age-related macular degeneration[35,36] and to lower the intraocular pressure in glaucoma.[37] Other research groups are also developing different types of nanoparticles to modulate wound healing in the eye.[38,39] Layer-by-layer nanoparticles (LbL-NPs) represent an efficient delivery vehicle for the siRNA silencing of secreted protein, acidic, and rich in cysteine (SPARC).[38] Cationic nano-copolymers combined with IKKβ siRNA [CS-g-(PEI-b-mPEG)/ IKKβ-siRNA] also increased bleb survival and decreased subconjunctival scarring in a monkey model of GFS.[39] There were no toxic side effects reported with the layer-by-layer nanoparticles and cationic nano-copolymers.

By designing a series of peptides, the goal was to understand how these different interactions affect gene delivery outcomes. Peptide Y was identified by biopanning a phage peptide library and closely resembles part of a targeting protein expressed by the intracellular pathogen Legionella pneumophila.[40,41] Although the identity of the receptor is still unknown, we have shown that peptide Y mediates the targeted delivery of siRNA in nanocomplexes to different tissues, including cells of neuronal origin,[41,42] lung cells,[22,28,43] primary vascular cells and rabbit

aorta.[40,44] ME27 is a cleavable peptide that contains a tripeptide Arg-Gly-Asp (RGD) motif that targets integrins, particularly $\alpha_v\beta_3$, $\alpha_v\beta_5$, and $\alpha_5\beta_1$, and these surface integrin receptors are abundantly expressed on human eye fibroblasts.[45]

The targeting peptide KG31 consists of a hydrophobic Y and KG32 contains a cleavable Y. We have previously synthesized peptides containing hydrophobic amino acids as spacers between a K_{16} moiety and an integrin-targeting motif. Our previous results had also shown that vectors containing peptides incorporating linkers that are partly hydrophobic demonstrated improved transfection properties, which is likely due to the improved accessibility of the integrin-binding motif.[46] We also hypothesized that by adding the cleavable linker RVRR in KG32, as is the case in peptide ME27, that this would promote processing of peptide components of receptor-targeted nanocomplex formulations. RVRR peptide motifs are cleavable by the endosomal enzymes furin and cathepsin B.[47] We have previously shown *in vitro* that peptides with cleavable linkers displayed improved transfection efficiencies compared to their non-cleavable peptide homologs.[47] The reason might be because endosomal cleavage of the peptides can lead to disengagement of the nanoparticle from the receptor, allowing more efficient release of the particle from the endosomal membrane, or removal of a peptide layer may make the particle smaller and thus more readily transported through the cytoplasm and the nuclear envelope.

In this study, cationic formulations using targeting peptides Y, ME27, KG31 and KG32 produced higher transfection efficiencies in human conjunctival fibroblasts than their non-targeting counterparts containing peptide ME72, suggesting receptor-specific transfection. Our previous study has also shown that receptor-targeted nanoparticles using peptides Y and ME27 achieved higher gene silencing efficiencies in transfecting conjunctival fibroblasts than nanoparticles with the non-targeting peptide K_{16} or with no peptides.[18] Even though the new targeting peptides KG31 and KG32 increased the transfection efficiency and *MRTF-B* gene silencing in human conjunctival fibroblasts compared to the non-targeting peptide, thereby supporting our above hypothesis, they however did not provide improved gene silencing over peptide Y.

Several studies have also reported a size-dependent cytotoxicity of nanoparticles.[48-50] In our study, LPRs containing DOTMA/DOPE lipid (DD) were around 120 nm with relatively low polydispersity index (0.37) and had no significant effect on cell viability in human conjunctival fibroblasts. On the other hand, LPRs containing DOTMA/DOPE + cholesterol lipid (DC) had significantly larger particle size (around 235 nm) and high polydispersity index (0.84), indicating a broad particle size distribution, and were cytotoxic to human conjunctival fibroblasts. LPRs containing anionic DOPG/DOPE + PEG lipid (DA) were around 102 nm with low polydispersity index (0.25) and had no significant effect on cell viability.[21,29]

Previous studies have shown increased targeted transfection efficiency, superior distribution and decreased inflammatory response of anionic PEGylated nanocomplexes *in vivo* compared to their homologous cationic formulations.[21,22,29] However, our results show that anionic PEGylated formulations did not have any significant effect *in vitro* on *MRTF-B* gene silencing in human conjunctival fibroblasts. One reason might be that the previous studies were conducted in cell lines as opposed to the primary human conjunctival fibroblasts used here. Therefore, on the basis of the *in vitro* silencing results, we did not progress to *in vivo* studies with the anionic formulations that could have shown possibly better silencing than those in the tissue culture studies and more comparable to that of the cationic counterparts. Future studies could involve the use of reduced PEGylation (e.g. 0.5%, 1%) to see whether that will enhance the silencing efficiency of anionic nanoparticles in human conjunctival fibroblasts.

Due to the positive zeta potential of *MRTF-B* LYR nanoparticles, interaction with proteins and other components *in vivo* can lead to aggregation. We did not observe any aggregation *in vivo* and we achieved a 29.6% *MRTF-B* gene silencing in rabbit conjunctival tissues after a single subconjunctival injection of MRTF-B LYR nanoparticles compared to control nanoparticles. This level of silencing was associated with an increase in bleb survival and a decrease in conjunctival scarring in a rabbit model of experimental GFS. MMC did not have any significant advantage over LYR nanoparticles. MMC works as an anti-scarring drug by causing widespread apoptosis of

fibroblasts and is not known to have an effect on the *MRTF-B* gene.[3] LYR design and dosage can also be further optimised and improved in future studies. We have previously shown that a 70% *MRTF-B* gene silencing in human conjunctival fibroblasts after a single transfection treatment completely blocked matrix contraction in a 7-day collagen contraction assay.[18]

One of the major challenges in developing novel anti-fibrotic drugs in GFS is to design long-acting drugs that would only need to be applied once at the time of surgery.[51] Future work will focus on optimising the best concentration and timing of injections to achieve long-acting and sustained gene silencing to prevent conjunctival fibrosis. For future clinical development, it will also be important to develop protocols for large-scale mixing of the lipid, peptide and siRNA components using Good Manufacturing Practice (GMP) materials and processes.[52,53] Such methods include microfluidic mixing and more standard, in-line mixing methodologies as reported for lipid and nucleic acid formulations.[54]

4. Conclusion

In this study, we have shown that receptor-targeted liposome-peptide-siRNA nanoparticles represent a safe and efficient siRNA delivery system that could be used to prolong bleb survival and to prevent conjunctival fibrosis after glaucoma filtration surgery, by targeting the *MRTF-B* gene as well as other potential gene targets associated with fibrosis.

5. Materials and Methods

Materials

1,2-di-O-octadecenyl-3-trimethylammonium propane (DOTMA), 1,2-dioleoyl-sn-glycero-3-phosphoethanolamine (DOPE), 1,2-dioleoyl-sn-glycero-3-phospho-(1'-rac-glycerol) (DOPG), 1,2-dipalmitoyl-sn-glycero-3-phosphoethanolamine-N-[methoxy(polyethylene glycol)-2000] (DPPE PEG2000) and cholesterol were purchased from Avanti Polar Lipids (Alabama, USA). The structures of the lipids, peptides and siRNAs are shown in Table 1. Peptides Y (K_{16}GACYGLPHKFCG), ME27 (K_{16}RVRRGACRGDCLG), ME72 (K_{16}RVRRGACRGECLG), KG31 (K_{16}RXSXGACYGLPHKFCG, Hydrophobic Y, X = epsilon-aminohexanoic acid), and KG32 (K_{16}RVRRGACYGLPHKFCG, Cleavable Y) were synthesized by ChinaPeptides (Shanghai, China) and AMS Biotechnology (Abingdon, UK). The siRNAs used in this study were custom-synthesized and purchased from Dharmacon (UK). The siRNAs were dissolved in sterile RNAse-free water at a concentration of 2.5 mg/ml.

Liposome preparation

Cationic liposomes made were: DOTMA: DOPE (DD) at 1:1 molar ratio and DOTMA: DOPE: Cholesterol (DC) at a molar ratio of 47.5: 47.5: 5 mol%. Anionic liposomes made were DOPG: DOPE: DPPE-PEG2000 (DA) at a molar ratio of 49.5: 49.5: 1 mol%. The lipids were dissolved in chloroform at 10 mg/ml and a lipid film was produced in a rotary evaporator by slowly evaporating the chloroform. Lipids were rehydrated with sterile RNAse-free water while constantly rotated overnight, and then sonicated in a water bath to reduce their size.

Cell culture

Human conjunctival fibroblasts were grown from donor human conjunctiva and informed consent was obtained from all subjects. Rabbit conjunctival fibroblasts were grown from New

Zealand white rabbit conjunctival tissues. The fibroblasts were maintained in Dulbecco's modified Eagle's medium (DMEM, Invitrogen) with 10% fetal calf bovine serum (FBS), 100 U/ml penicillin, 100 mg/ml streptomycin, and 2 nM L-glutamine, in tissue culture incubators with 5% CO_2 and 95% humidity. Fibroblasts between passages 2-8 were used in the experiments. All experimental protocols were approved by the London-Dulwich Research Ethics Committee (REC 10/H0808/127) and the institutional approval committee at the University College London Institute of Ophthalmology.

Nanoparticle formulation

LPRs containing DOTMA/DOPE (DD) and LPRs containing DOTMA/DOPE + cholesterol (DC) were prepared at a weight ratio of 1 (liposome): 4 (peptide): 1 (siRNA), by first mixing the liposome with the peptide, followed by the addition of siRNA. The mixture was incubated at room temperature (25°C) for one hour to allow complex formation. OptiMEM **(**Life Technologies, UK**)** was then added to give a final siRNA concentration of 50 nM. LPRs containing DOPG/DOPE + anionic PEG (DA) were prepared at a weight ratio of 19 (liposome): 2.7 (peptide): 1 (siRNA), by first mixing the peptide with the siRNA and incubating for 30 minutes at room temperature. The liposome was then mixed with the peptide-siRNA and incubated for a further 30 minutes.

Nanoparticle size and zeta potential

Nanoparticle size and zeta potential were determined by dynamic light scattering (DLS) and laser Doppler anemometry, respectively, using a Nano ZS Zetasizer (Malvern Instruments, Malvern, UK) with the following specifications: automatic sampling time of 10 measurements/ sample, refractive index of 1.330, dielectric constant 78.5, viscosity 0.8872 cP, and temperature of 25°C. Zeta potential settings were calibrated against the standard (-68 ± 6.8 mV). Triplicate measurements were performed for each sample and the results were analysed using the software provided by the manufacturer (DTS version 5.03).

Transmission Electron Microscopy (TEM)

The nanoparticles were applied onto a 300-mesh copper grid coated with a Formvar/ carbon support film (Agar Scientific, Stansted, UK) and processed as previously described [21]. The samples were negatively stained with 1% uranyl acetate for 2-3 seconds, before blotting with filter paper and air-drying. Imaging was performed with a Philips CM120 BioTwin Transmission Electron Microscope and operated at an accelerating voltage of 120 kV. Images were captured using an AMT 5MP digital TEMcamera (Deben UK Limited, Suffolk, UK).

***In vitro* transfection**

The human and rabbit conjunctival fibroblasts were seeded at 1 x 10^5 cells/ well in 6-well plates (Falcon, Fisher Scientific UK) and incubated for 24 hours before the nanocomplexes were added. The cells were incubated with the nanocomplexes in OptiMEM for 4 hours at 37°C. The medium containing the nanocomplexes was then replaced by fresh growth medium and the cells were incubated for a further 48 hours at 37°C.

Real-Time Quantitative PCR

The human and rabbit conjunctival fibroblasts were lysed for RNA extraction using the RNeasy mini kit (Qiagen, UK) according to the manufacturer's instructions. The rabbit conjunctival tissues were mechanically dispersed and RNA was also extracted using the RNeasy mini kit (Qiagen, UK). RT-qPCR reactions were performed using a SensiFAST^{TM} SYBR Hi-ROX One-Step master mix (Bioline, UK) on a CFX Real-Time PCR detection system (Bio-Rad, Hemel Hempstead, UK). The qRT-PCR assay conditions were: stage 1, 45°C for 20 minutes; stage 2, 95°C for 3 minutes; stage 3, 95°C for 10 seconds, then 60°C for 25 seconds; repeated 40 times. The human Taqman gene expression assays were MRTF-B/MKL2 (Hs00401867_m1) and GAPDH (Hs02758991_g1) (ThermoFisher Scientific, UK). The rabbit primers were: MRTF-B, 5'-

CTCCGATGTGGGTTTATGGGT-3', 3'-GGAAGTGGCATCAGGACAGT-5'; ACTA2, 5'-TCCACCGCAAATGCTTCTAAGT-3', 3'-ATGAGTCAGAGCTTTGGATAGGC-5'; GAPDH, 5'-CGAGACACGATGGTGAAGGT-3', 3'-CCAGCATCACCCCACTTGAT-5'. All mRNA values were normalized relative to that of GAPDH and triplicate experiments were performed for each condition.

Cell proliferation assay

The human and rabbit conjunctival fibroblasts were seeded at 0.625 x 10^4 cells/ well in 96-well plates (Falcon, Fisher Scientific UK). The cells were transfected with six replicates for each nanoparticle formulation and cell viability was measured using the Cell Titer 96 Aqueous one solution cell proliferation assay (Promega, UK). The medium was replaced with 100 µl fresh growth medium per well and 20 µl of the Cell Titer 96 Aqueous one solution were added to each well. The cells were incubated for 2 hours and absorbance at 540 nm was measured using a FLUOstar Optima (BMG LABTECH). Cell viability for each formulation was expressed as a percentage of the viability of control cells.

Rabbit glaucoma filtration surgery (GFS) model of scar tissue formation

All animal procedures were performed in accordance with the Association of Research in Vision and Ophthalmology (ARVO) Statement for the Use of Animals in Ophthalmic and Vision Research, and all animal experimental protocols were approved by the Home Office UK (PPL 70/8074). Eighteen female New Zealand white rabbits (1.5-2 kg, 10-12 weeks, Envigo, UK) underwent experimental GFS to the left eye under general anaesthesia [25,26]. A superonasal fornix-based conjunctival flap was raised behind the limbus and a micro-vitreoretinal blade (20 gauge, 0.90 mm, Surgistar USA) was used to make a partial thickness scleral tunnel to the corneal stroma. A 22 gauge, 25 mm intravenous cannula was passed through the tunnel and the needle was removed once it was visible in the cornea. The cannula was advanced into the mid-pupillary area,

trimmed at its scleral edge and fixed to the scleral surface using a 10-0 nylon suture (Alcon, USA). The conjunctival incision was closed using two interrupted 10-0 nylon sutures. In a randomised, prospective, single-masked observer study, the rabbits received intraoperative 0.2 mg/ml mitomycin-C [N=6] or a postoperative subconjunctival injection of 25 μg in 100 μl of MRTF-B LYR nanoparticles [N=6] or control LYR nanoparticles [N=6].

Post-operative clinical examination

The animals were examined every 3 days by a single-masked blinded researcher. Bleb width and length were measured using calipers and intraocular pressures were measured using a tonovet (Icare, UK). The primary efficacy end-point was bleb survival as this is indicative of the long-term patency of the filtration pathway created during surgery. Bleb failure was defined as the appearance of a flat, scarred, and vascularised bleb associated with a deep anterior chamber. All animals were also evaluated for signs of local or systemic toxicity during the study.

Histologic analysis

The animals were sacrificed on day 30 and both eyes were enucleated. The eyes were fixed in formalin, embedded in paraffin, and sequential 4 μm tissue sections were cut. The sections were stained with hematoxylin and eosin (for cellularity and inflammatory cells), Gomori's trichrome (for collagen), picrosirius red (for degree of fibrosis), and alpha-smooth muscle actin (αSMA) using a primary monoclonal mouse anti-human αSMA antibody (Clone 1A4; Dako, High Wycombe, UK) and a biotinylated secondary antibody (rabbit anti-mouse; Dako). All the left operated eyes were compared to the right non-operated eyes that were used as controls for normal conjunctival tissue.

Statistical analysis

All graphs display mean and standard error of the mean (SEM). Statistical analysis was performed using the Student's t-test to calculate statistically significant differences and *p* values. Survival analysis for bleb was performed using the Kaplan-Meier log rank test. Statistically significant differences were expressed as *, $p < 0.05$; **, $p < 0.01$; ***, $p < 0.001$.

References

1 Tham, Y. C. *et al.* Global prevalence of glaucoma and projections of glaucoma burden through 2040: a systematic review and meta-analysis. *Ophthalmology* **121**, 2081-2090 (2014).

2 Addicks, E. M., Quigley, H. A., Green, W. R. & Robin, A. L. Histologic characteristics of filtering blebs in glaucomatous eyes. *Arch Ophthalmol* **101**, 795-798 (1983).

3 Crowston, J. G. *et al.* Antimetabolites-induced apoptosis in Tenon's capsule fibroblasts. *Invest Ophthalmol Vis Sci.* **39**, 449-454 (1998).

4 Singh, J., O'Brien, C. & Chawla, H. B. Success rate and complications of intraoperative 0.2 mg/ml mitomycin C in trabeculectomy surgery. *Eye (Lond)* **9**, 460-466 (1995).

5 Parrish, R. & Minckler, D. "Late endophthalmitis": Filtering surgery time bomb? *Ophthalmology.* **103**, 1167-1168 (1996).

,6 Dougherty, P. J., Hardten, D. R. & Lindstrom, R. L. Corneoscleral melt after pterygium surgery using a single intraoperative application of mitomycin-C. *Cornea* **15**, 537-540 (1996).

7 Rubinfeld, R. S. *et al.* Serious complications of topical mitomycin-C after pterygium surgery. *Ophthalmology* **99**, 1647-1654 (1992).

8 Esnault, C. *et al.* Rho–actin signaling to the MRTF coactivators dominates the immediate transcriptional response to serum in fibroblasts. *Genes Dev.* **28**, 943-958 (2014).

9 Olson, E. N. & Nordheim, A. Linking actin dynamics and gene transcription to drive cellular motile functions. *Nat Rev Mol Cell Biol.* **11**, 353-365 (2010).

10 Minami, T. *et al.* Reciprocal expression of MRTF-A and myocardin is crucial for pathological vascular remodelling in mice. *EMBO J* **31**, 4428-4440 (2012).

11 Haak, A. J. *et al.* Targeting the myofibroblast genetic switch: inhibitors of MRTF/SRF-regulated gene transcription prevent fibrosis in a murine model of skin injury. *J Pharmacol Exp Ther*. **349**, 480-486 (2014).

12 Sisson, T. H. *et al.* Inhibition of Myocardin-Related Transcription Factor/Serum Response Factor Signaling Decreases Lung Fibrosis and Promotes Mesenchymal Cell Apoptosis. *Am J Pathol.* **185**, 969-986 (2015).

13 Posern, G. & Treisman, R. Actin' together: serum response factor, its cofactors and the link to signal transduction. *Trends Cell Biol.* **16**, 588-596 (2006).

14 Vartiainen, M. K., Guettler, S., Larijani, B. & Treisman, R. Nuclear actin regulates dynamic subcellular localization and activity of the SRF cofactor MAL. *Science* **316**, 1749-1752 (2007).

15 Miralles, F., Posern, G., Zaromytidou, A. I. & Treisman, R. Actin dynamics control SRF activity by regulation of its coactivator MAL. *Cell* **113**, 329-342 (2003).

16 Yu-Wai-Man, C. *et al.* Genome-wide RNA-Sequencing analysis identifies a distinct fibrosis gene signature in the conjunctiva after glaucoma surgery. *Sci Rep* **7**, 5644 (2017).

17 Yu-Wai-Man, C. *et al.* Local delivery of novel MRTF/SRF inhibitors prevents scar tissue formation in a preclinical model of fibrosis. *Sci Rep.* **7**, 518 (2017).

18 Yu-Wai-Man, C., Tagalakis, A. D., Manunta, M. D., Hart, S. L. & Khaw, P. T. Receptor-targeted liposome-peptide-siRNA nanoparticles represent an efficient delivery system for MRTF silencing in conjunctival fibrosis. *Sci Rep.* **6**, 21881 (2016).

19 Yu-Wai-Man, C., Treisman, R., Khaw, P. T. & Bailly, M. Targeting the MRTF/SRF gene transcription pathway in conjunctival fibrosis in glaucoma. *Lancet* **387**, S111. doi: 110.1016/S0140-6736(1016)00498-00490 (2016).

20 Elbashir, S. M. *et al.* Duplexes of 21-nucleotide RNAs mediate RNA interference in cultured mammalian cells. *Nature* **411**, 494-498 (2001).

21 Tagalakis, A. D. *et al.* PEGylation improves the receptor-mediated transfection efficiency of peptide-targeted, self-assembling, anionic nanocomplexes. *J Control Release* **174**, 177-187 (2014).

22 Tagalakis, A. D. *et al.* Multifunctional, self-assembling anionic peptide-lipid nanocomplexes for targeted siRNA delivery. *Biomaterials* **35**, 8406-8415 (2014).

23 Liu, Y. *et al.* Factors influencing the efficiency of cationic liposome-mediated intravenous gene delivery. *Nat Biotechnol.* **15**, 167-173 (1997).

24 Liu, Y. *et al.* Cationic liposome-mediated intravenous gene delivery. *J Biol Chem.* **270**, 24864-24870 (1995).

25 Cordeiro, M. F., Gay, J. & Khaw, P. T. Human anti-transforming growth factor-beta2 antibody: a new glaucoma anti-scarring agent. *Invest Ophthalmol Vis Sci* **40**, 2225-2234 (1999).

26 Wong, T. T. L., Mead, A. L. & Khaw, P. T. Matrix Metalloproteinase Inhibition Modulates Postoperative Scarring after Experimental Glaucoma Filtration Surgery. *Invest Ophthalmol Vis Sci.* **44**, 1097-1103 (2003).

27 Kenny, G. D. *et al.* Multifunctional receptor-targeted nanocomplexes for magnetic resonance imaging and transfection of tumours. *Biomaterials* **33**, 7241-7250 (2012).

28 Tagalakis, A. D. *et al.* Peptide and nucleic acid-directed self-assembly of cationic nanovehicles through giant unilamellar vesicle modification: Targetable nanocomplexes for in vivo nucleic acid delivery. *Acta Biomater.* **51**, 351-362 (2017).

29 Kenny, G. D. *et al.* Multifunctional receptor-targeted nanocomplexes for the delivery of therapeutic nucleic acids to the brain. *Biomaterials* **34**, 9190-9200 (2013).

30 Draz, M. S. *et al.* Nanoparticle-mediated systemic delivery of siRNA for treatment of cancers and viral infections. *Theranostics* **4**, 872-892 (2014).

31 Kim, B. *et al.* Inhibition of ocular angiogenesis by siRNA targeting vascular endothelial growth factor pathway genes - therapeutic strategy for herpetic stromal keratitis. *Am J Pathol* **165**, 2177-2185 (2004).

32 Jia, R. B. *et al.* VEGF-targeted RNA interference suppresses angiogenesis and tumor growth of retinoblastoma. *Ophthalmic Res.* **39**, 108-115 (2007).

33 Nakamura, H. *et al.* RNA interference targeting transforming growth factor-beta type II receptor suppresses ocular inflammation and fibrosis. *Mol Vis* **10**, 703-711 (2004).

34 Solano, E. C. *et al.* Toxicological and pharmacokinetic properties of QPI-1007, a chemically modified synthetic siRNA targeting caspase 2 mRNA, following intravitreal injection. *Nucleic Acid Ther.* **24**, 258-266 (2014).

35 Nguyen, Q. D. *et al.* Evaluation of the siRNA PF-04523655 versus ranibizumab for the treatment of neovascular age-related macular degeneration (MONET Study). *Ophthalmology* **119**, 1867-1873 (2012).

36 Kaiser, P. K. *et al.* RNAi-Based Treatment for Neovascular Age-Related Macular Degeneration by Sirna-027. *Am J Ophthalmol* **150**, 33-39 (2010).

37 Martínez, T. *et al.* In vitro and in vivo efficacy of SYL040012, a novel siRNA compound for treatment of glaucoma. *Mol Ther.* **22**, 81-91 (2014).

38 Tan, Y. F. *et al.* Layer-by-layer nanoparticles as an efficient siRNA delivery vehicle for SPARC silencing. *Small* **10**, 1790-1798 (2014).

39 Ye, H. *et al.* Cationic nano-copolymers mediated IKKβ targeting siRNA to modulate wound healing in a monkey model of glaucoma filtration surgery. *Mol Vis.* **16**, 2502-2510 (2010).

40 Irvine, S. A. *et al.* Receptor-targeted nanocomplexes optimized for gene transfer to primary vascular cells and explant cultures of rabbit aorta. *Mol. Ther.* **16**, 508-515 (2008).

41 Tagalakis, A. D., He, L., Saraiva, L., Gustafsson, K. T. & Hart, S. L. Receptor-targeted liposome-peptide nanocomplexes for siRNA delivery. *Biomaterials* **32**, 6302-6315 (2011).

42 Tagalakis, A. D., Saraiva, L., McCarthy, D., Gustafsson, K. T. & Hart, S. L. Comparison of nanocomplexes with branched and linear peptides for siRNA delivery. *Biomacromolecules* **14**, 761-770 (2013).

43 Tagalakis, A. D. *et al.* A method for concentrating lipid peptide DNA and siRNA nanocomplexes that retains their structure and transfection efficiency. *Int J Nanomedicine* **10**, 2673-2683 (2015).

44 Meng, Q. H. *et al.* Inhibition of neointimal hyperplasia in a rabbit vein graft model following non-viral transfection with human iNOS cDNA. *Gene Ther.* **20**, 979-986 (2013).

45 Masur, S. K., Cheung, J. K. H. & Antohi, S. Identification of Integrins in Cultured Corneal Fibroblasts and in Isolated Keratocytes. *Invest Ophthalmol Vis Sci* **34**, 2690-2698 (1993).

46 Pilkington-Miksa, M. A. *et al.* Targeting lipopolyplexes using bifunctional peptides incorporating hydrophobic spacer amino acids: synthesis, transfection, and biophysical studies. *Bioconjug Chem.* **18**, 1800-1810 (2007).

47 Grosse, S. M. *et al.* Tumor-specific gene transfer with receptor-mediated nanocomplexes modified by polyethylene glycol shielding and endosomally cleavable lipid and peptide linkers. *FASEB J* **24**, 2301-2313 (2010).

48 Carlson, C. *et al.* Unique cellular interaction of silver nanoparticles: size-dependent generation of reactive oxygen species. *J Phys Chem B.* **112**, 13608-13619 (2008).

49 Pan, Y. *et al.* Size-dependent cytotoxicity of gold nanoparticles. *Small.* **3**, 1941-1949 (2007).

50 Prabhu, B. M., Ali, S. F., Murdock, R. C., Hussain, S. M. & Srivatsan, M. Copper nanoparticles exert size and concentration dependent toxicity on somatosensory neurons of rat. *Nanotoxicology.* **4**, 150-160 (2010).

51 Yu-Wai-Man, C. & Khaw, P. T. Developing novel anti-fibrotic therapeutics to modulate post-surgical wound healing in glaucoma: Big potential for small molecules. *Expert Rev Ophthalmol.* **10**, 65-76 (2015).

52 Wittrup, A. & Lieberman, J. Knocking down disease: a progress report on siRNA therapeutics. *Nat Rev Genet.* **16**, 543-552 (2015).

53 Rizk, M. & Tüzmen, Ş. Update on the clinical utility of an RNA interference-based treatment: focus on Patisiran. *Pharmgenomics Pers Med.* **10**, 267-278 (2017).

54 Walsh, C. *et al.* Microfluidic-based manufacture of siRNA-lipid nanoparticles for therapeutic applications. *Methods Mol Biol.* **1141**, 109-120 (2014).

Acknowledgements:

Our research is supported by the National Institute for Health Research (NIHR) Biomedical Research Centre at Moorfields Eye Hospital NHS Foundation Trust and UCL Institute of Ophthalmology, the Medical Research Council (Grant 535333) and Moorfields Eye Charity. This work was also supported by the National Institute for Health Research Biomedical Research Centre at Great Ormond Street Hospital for Children NHS Foundation Trust and University College London.

Author contributions:

CY designed the experiments, supervised staff, conducted the research and wrote the manuscript. OF, AT and SA performed the experiments, analysed the data and contributed to the manuscript. SH, PTK and SB contributed to the research and to the manuscript.

Conflict of interests:

The authors declare that they have no conflict of interest.

Figure Legends

Figure 1. Biophysical characterisation of multiple lipid-peptide-human siRNA nanoparticle formulations. **(A)** Size in nm. **(B)** Zeta potential in mV. **(C)** Polydispersity index. Results represent mean ± SEM. **(D)** Negative staining transmission electron microscopy. Scale bar = 200 nm. DD, DOTMA/DOPE; DC, DOTMA/DOPE + cholesterol; DA, anionic DOPG/DOPE + PEG; Targeting peptides Y, ME27, KG31, KG32; Non-targeting peptide ME72; R, siRNA.

Figure 2. *In vitro* transfections of human conjunctival fibroblasts and *MRTF-B* gene silencing by lipid-peptide-siRNA (LPR) nanoparticles. **(A)** LPRs containing DOTMA/DOPE lipid (DD). **(B)** LPRs containing DOTMA/DOPE + cholesterol lipid (DC). **(C)** LPRs containing anionic DOPG/DOPE + PEG lipid (DA). mRNA levels were normalized relative to that of GAPDH and the results represent mean ± SEM for triplicate experiments. *, $p < 0.05$; **, $p < 0.01$; ***, $p < 0.001$.

Figure 3. Viability of human conjunctival fibroblasts after transfection with lipid-peptide-siRNA (LPR) nanoparticles for 48 hours. **(A)** LPRs containing DOTMA/DOPE lipid (DD). **(B)** LPRs containing DOTMA/DOPE + cholesterol lipid (DC). **(C)** LPRs containing anionic DOPG/DOPE + PEG lipid (DA). Results represent mean ± SEM for six independent replicates. *, $p < 0.05$; **, $p < 0.01$.

Figure 4. *In vitro* transfections of rabbit conjunctival fibroblasts using LPR formulations of DOTMA/DOPE with the targeting peptide Y and rabbit siRNA sequences (LYR). **(A)** Size in nm. **(B)** Zeta potential in mV. Results represent mean ± SEM. **(C)** mRNA levels were normalized relative to that of GAPDH and the results represent mean ± SEM for triplicate experiments. *, $p < 0.05$. **(D)** Cell viability after transfection for 48 hours. Results represent mean ± SEM for six independent replicates.

Figure 5. Effect of LYR nanoparticle formulations on a rabbit model of glaucoma filtration surgery. **(A)** Schematic diagram to illustrate aqueous fluid draining through inserted filtration cannula and subconjunctival administration of nanocomplexes. **(B)** Morphology of blebs after surgery and treatment with MRTF-B LYR nanoparticles, control nanoparticles, or mitomycin-C (MMC). Arrows indicate bleb edges. **(C)** Kaplan-Meier graph comparing the bleb survival between MRTF-B LYR nanoparticles [N=6], control LYR nanoparticles [N=6], and MMC [N=6].

Figure 6. Histology of rabbit conjunctival tissues. The left operated eyes were compared to the right non-operated eyes that were used as controls for normal conjunctival tissue. Scale bar = 100 μm; c, conjunctiva, b, subconjunctival space, s, sclera. **(A)** Picrosirius red; **(B)** H&E; **(C)** αSMA; **(D)** Gomori's trichrome stain.

Figure 7. Gene silencing of **(A)** *MRTF-B* and **(B)** *ACTA2* in rabbit conjunctival tissues after subconjunctival injection of MRTF-B LYR nanoparticles. mRNA levels were normalized relative to that of GAPDH and the results represent mean ± SEM for triplicate experiments. *, $p < 0.05$.

Table Legends

Table 1. Structures of the different lipids and sequences of peptides and siRNAs

Function	Lipids	Structure
Cationic Lipid Structure	DOTMA [1,2-di-O-octadecenyl-3-trimethylammonium propane]	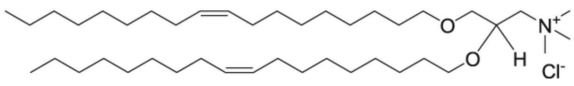
Helper Lipid	DOPE [1,2-dioleoyl-sn-glycero-3-phosphoethanolamine]	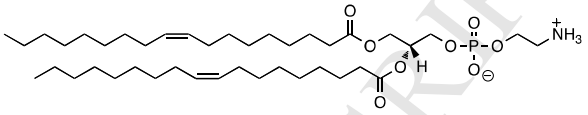
Helper Lipid	Cholesterol	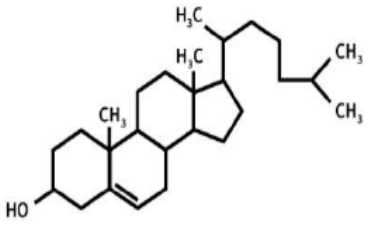
Anionic Lipid Structure	DOPG [1,2-dioleoyl-*sn*-glycero-3-phospho-(1'-*rac*-glycerol)]	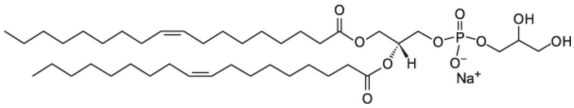
Function	**Peptides**	**Sequence**
Targeting	Y	K_{16}GACYGLPHKFCG
Targeting	ME27	K_{16}RVRRGACRGDCLG
Non-Targeting	ME72	K_{16}RVRRGACRGECLG
Targeting	KG31	K_{16}RXSXGACYGLPHKFCG (Hydrophobic Y), where X = epsilon-aminohexanoic acid
Targeting	KG32	K_{16}RVRRGACYGLPHKFCG (Cleavable Y)
Function	**siRNAs**	**Sequence**
Targeting	MRTF-B (Human)	GGAUGGAACUUUACCCUCA
Targeting	MRTF-B (Rabbit)	CGAGAAAGGUGUUCACAAAUU
Non-Targeting	Control	UGGUUUACAUGUCGACUAA

RNA interference induced by double-stranded, small interfering RNA (siRNA) is a naturally-occurring approach to silence gene expression with high specificity. Yu-Wai-Man and colleagues show that lipid-peptide-siRNA (LPR) nanoparticles significantly increase bleb survival and prevent conjunctival fibrosis in a pre-clinical model of glaucoma filtration surgery.

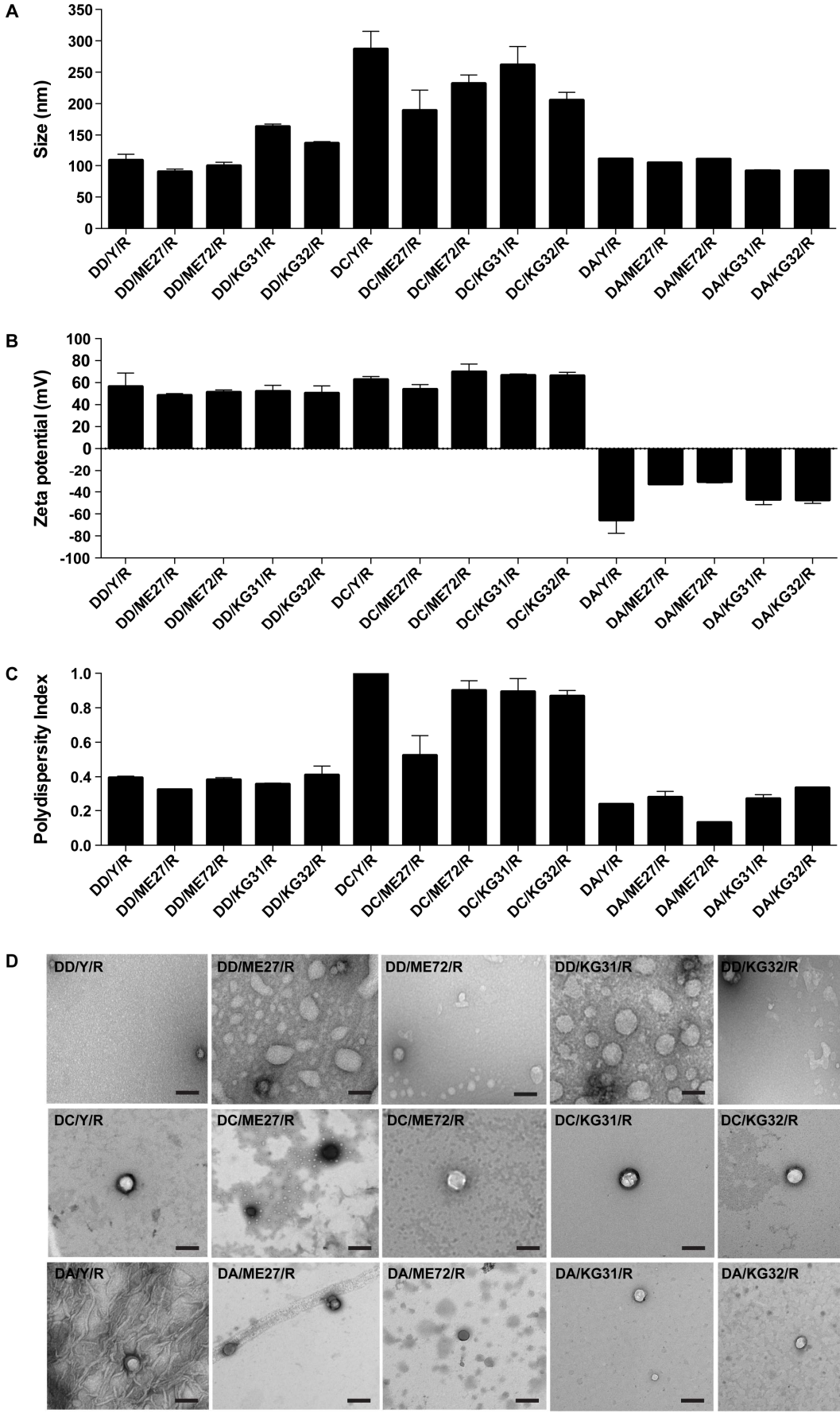
A
Size (nm)
350
300
250
200
150
100
50
0
DD/Y/R
DD/ME27/R
DD/ME72/R
DD/KG31/R
DD/KG32/R
DC/Y/R
DC/ME27/R
DC/ME72/R
DC/KG31/R
DC/KG32/R
DA/Y/R
DA/ME27/R
DA/ME72/R
DA/KG31/R
DA/KG32/R
B
Zeta potential (mV)
100
80
60
40
20
0
-20
-40
-60
-80
-100
C
Polydispersity Index
1.0
0.8
0.6
0.4
0.2
0.0
D

A

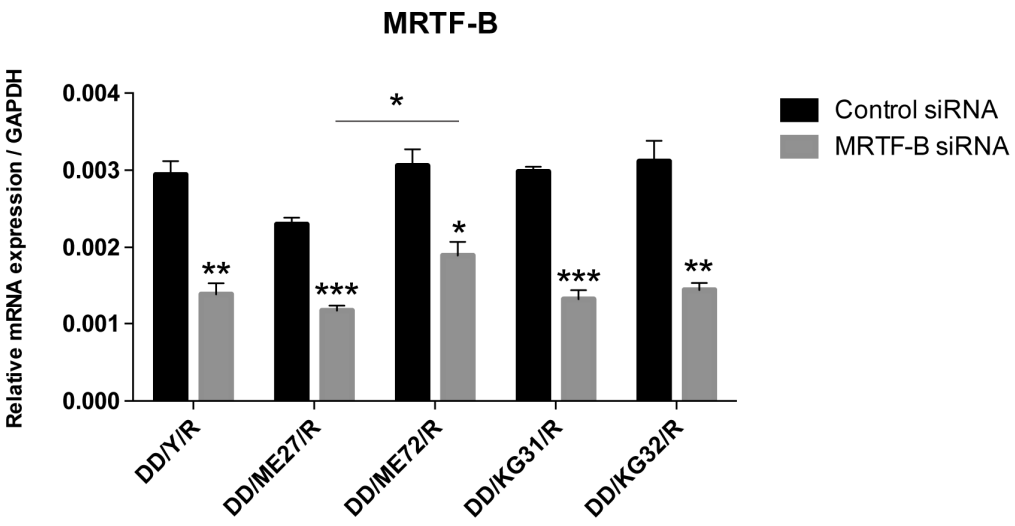
MRTF-B
Relative mRNA expression / GAPDH
0.004
0.003
0.002
0.001
0.000
Control siRNA
MRTF-B siRNA
DD/Y/R
DD/ME27/R
DD/ME72/R
DD/KG31/R
DD/KG32/R

B

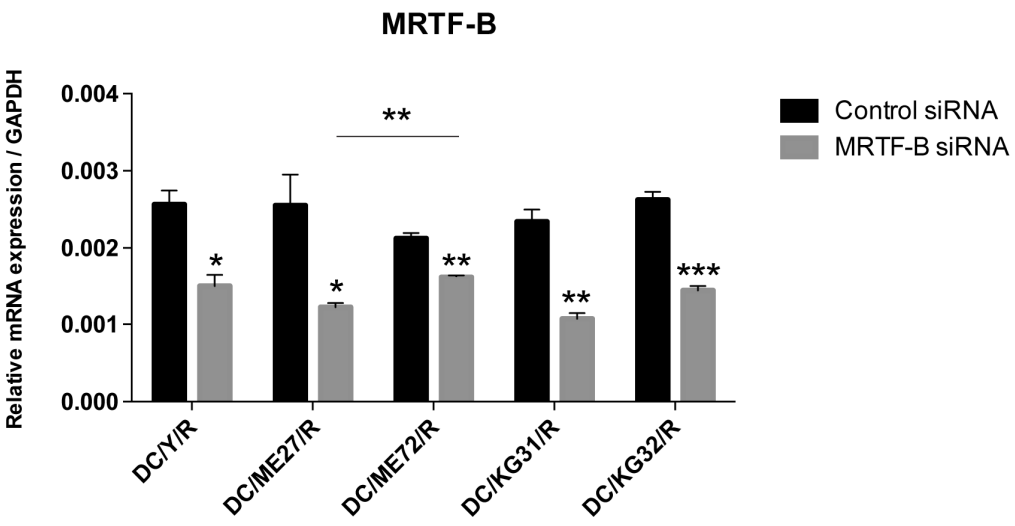
MRTF-B
Relative mRNA expression / GAPDH
0.004
0.003
0.002
0.001
0.000
Control siRNA
MRTF-B siRNA
DC/Y/R
DC/ME27/R
DC/ME72/R
DC/KG31/R
DC/KG32/R

C

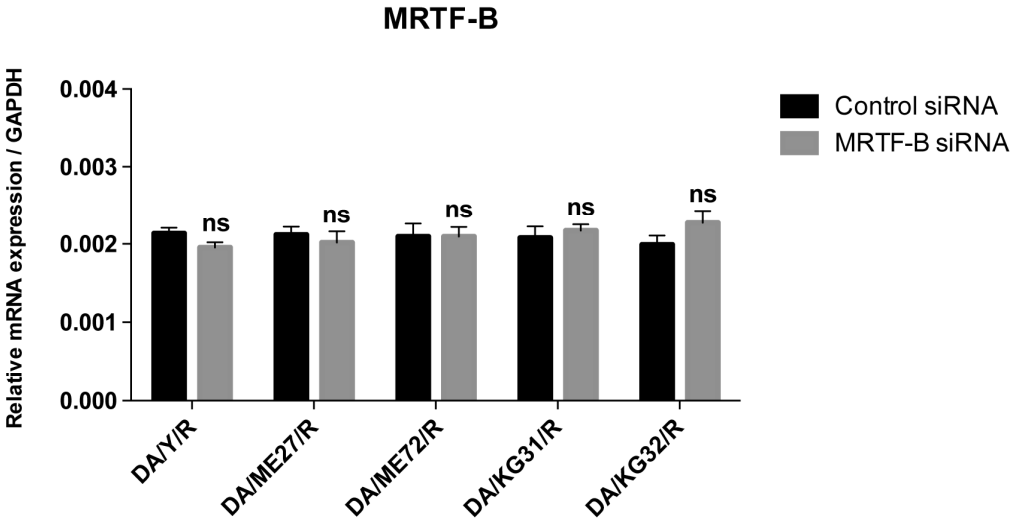
MRTF-B
Relative mRNA expression / GAPDH
0.004
0.003
0.002
0.001
0.000
Control siRNA
MRTF-B siRNA
DA/Y/R
DA/ME27/R
DA/ME72/R
DA/KG31/R
DA/KG32/R

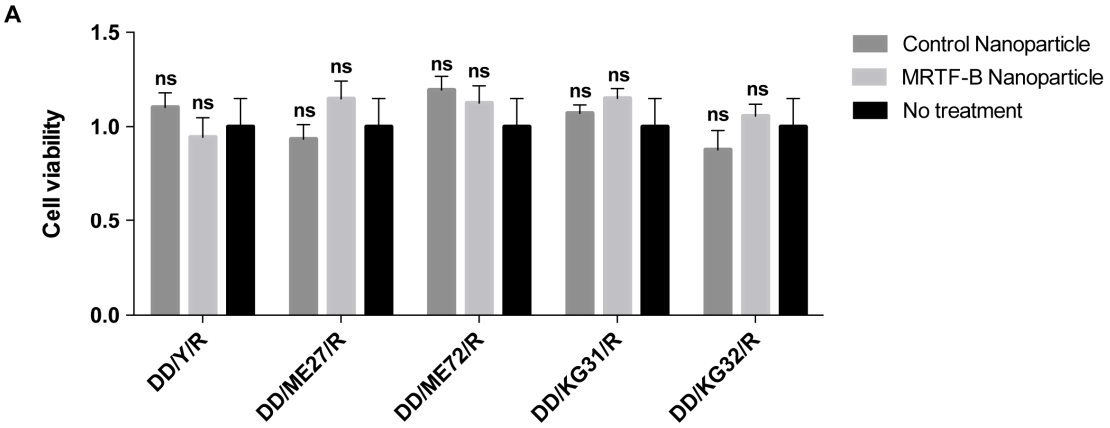
A
Cell viability
1.5
1.0
0.5
0.0
ns
DD/Y/R
DD/ME27/R
DD/ME72/R
DD/KG31/R
DD/KG32/R
Control Nanoparticle
MRTF-B Nanoparticle
No treatment

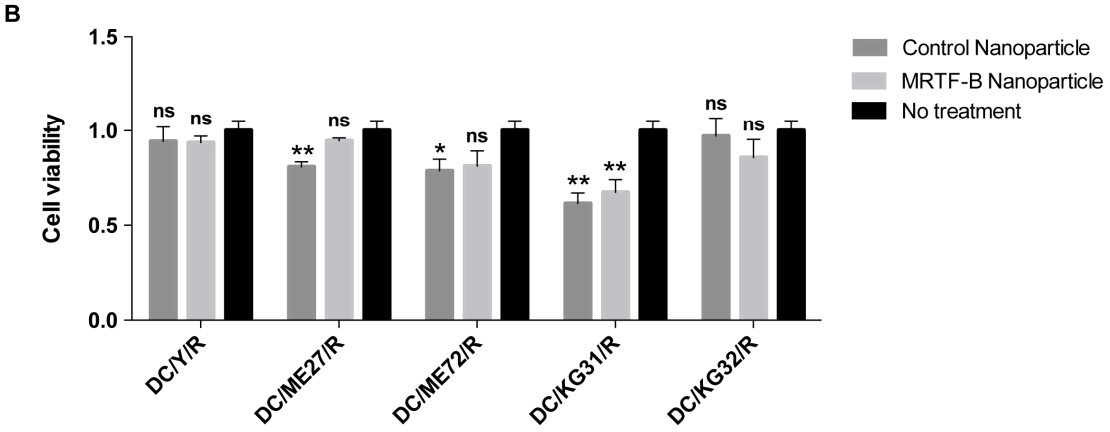
B
Cell viability
1.5
1.0
0.5
0.0
ns
**
*
DC/Y/R
DC/ME27/R
DC/ME72/R
DC/KG31/R
DC/KG32/R
Control Nanoparticle
MRTF-B Nanoparticle
No treatment

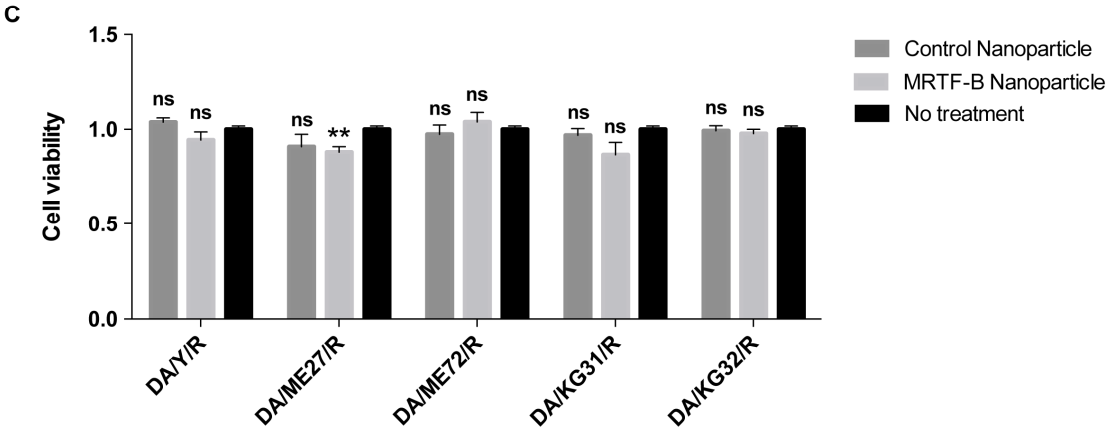
C
Cell viability
1.5
1.0
0.5
0.0
ns
**
DA/Y/R
DA/ME27/R
DA/ME72/R
DA/KG31/R
DA/KG32/R
Control Nanoparticle
MRTF-B Nanoparticle
No treatment

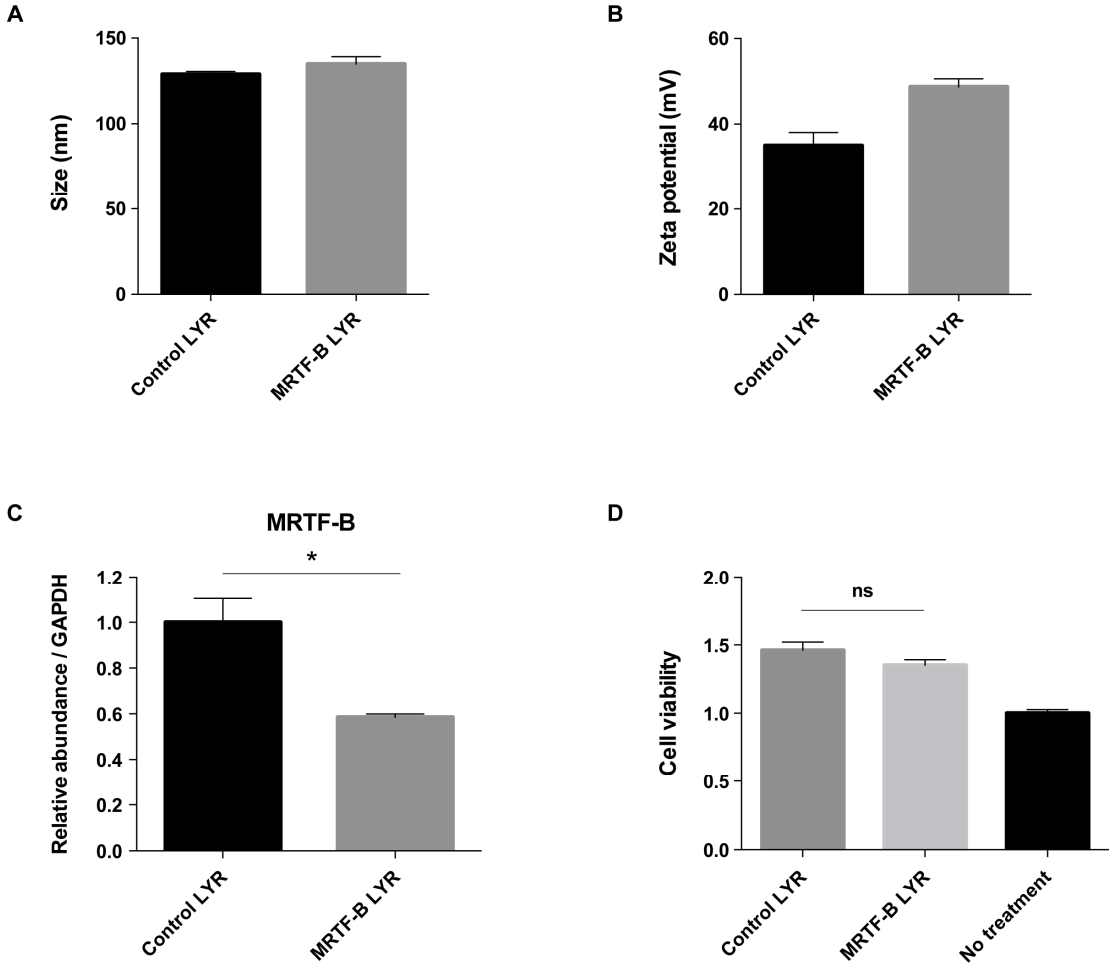

A

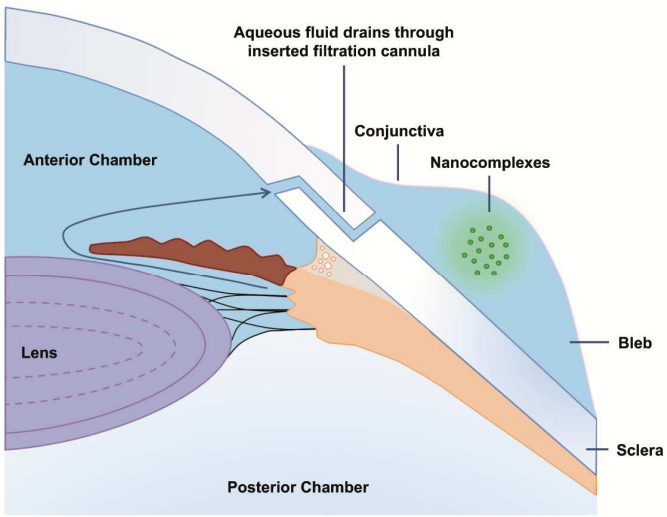
Aqueous fluid drains through inserted filtration cannula
Conjunctiva
Nanocomplexes
Anterior Chamber
Lens
Bleb
Sclera
Posterior Chamber

B

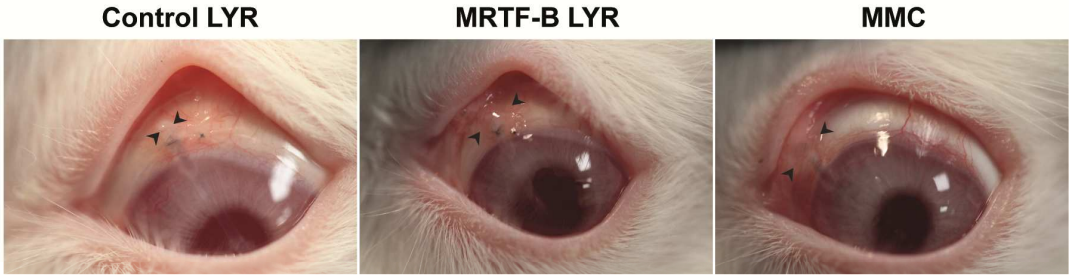
Control LYR
MRTF-B LYR
MMC

C

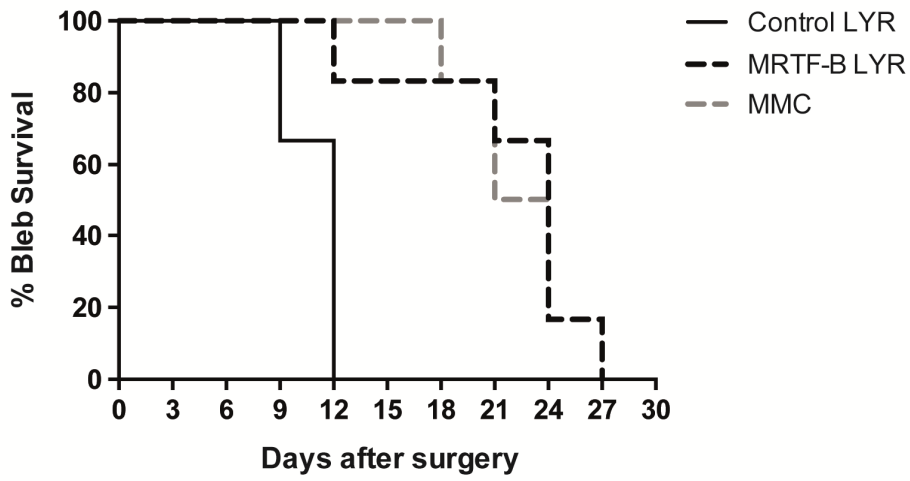
% Bleb Survival
100
80
60
40
20
0
0 3 6 9 12 15 18 21 24 27 30
Days after surgery
Control LYR
MRTF-B LYR
MMC